Kufa Journal of Engineering
Vol. 17, No. 1, January 2026, P.P. 272-290
Article history: Received 1 March 2025, last revised 25 March 2025, accepted 5 April 2025

USING THE ADAPTIVERANDOARMASKAUGMENTATION FUNCTION FOR MEDICAL IMAGE AUGMENTATION AND MASK INPAINTING WITH DEEP LEARNING

Zainab Adnan Jwad[1] and Israa Hadi Ali[2]

[1] PhD student, Department of Software, College of Information Technology, University of Babylon, Babylon, Iraq, Email:inf302.zanab.adnan@student.uobabylon.edu.iq.

[2] Professor, Dr., Department of Software, College of Information Technology, University of Babylon, Babylon, Iraq, Email:Iraq israa_hadi@itnet.uobabylon.edu.iq.

https://doi.org/10.30572/2018/KJE/170115

ABSTRACT

The segmentation of medical images via deep learning is troubled by two primary issues: lack of segmented data and difficulty of shapes. Modern approaches for data augmentation have clearly surpassed classical techniques like shifting, rotating and flipping in terms of performance. The AdaptiveRandOARMaskAugmentation method implements elastic deformations alongside dynamic deformations and intelligent edge noise injection to develop authentic anatomical changes in training data. This method has been deployed within the MONAI framework because it enables interoperability for deep learning systems. The approach outperformed traditional approaches by obtaining a 7.4% Dice score enhancement alongside a 2.9 mm reduction of HD95 on OpenKBP radiological planning dataset tests. The method retained its 12% accuracy decrease when elastic deformation was severed from testing procedures. The research shows the promising practical value of this approach for radiological planning since it boosts reliable critical organ recognition performance across anatomically comparable areas. The technique solves both incomplete data problems and class distribution problems to improve model outcomes for real-world applications.

KEYWORDS

Data augmentation, Deep learning, Medical Image, Dice score, Elastic deformation, Morphological operation, Noise injection.

1. INTRODUCTION

Medical imaging research faces significant barriers when establishing deep learning models for image segmentation because of limited labeled data availability and anatomical structure complexity (Mohammed, Kareem and Mohammed, 2022). The development of virtual dataset expansion became a necessary measure to cope with such challenges by data augmentation (Legrand et al., 2024). The classical approaches to image augmentation (such as rotation scale changes and flipping) are applicable on a large scale but cannot satisfy the demands of medical imaging activities. The distortions in the application of these methods to anatomical fidelity include its use in producing segmentation masks, especially in OAR delineation in a CT scan, where fine spatial imaging and detailed morphological data are required (Kamnitsas et al., 2018; Jwad and Ali, 2025) Moreover, the conventional methods impose the same transformation on all the data samples without taking into account anatomical context, which leads to augmented images that do not recap natural biological variability and are incapable of modeling clinically relevant morphological variation (Fadel, Abbood and Gheni, 2022). Traditionally used methods for processing mask data do not consider many of the complex changes that occur during image segmentation so therefore a specialized piece of equipment is needed to represent anatomically and otherwise accurately. This research introduces the AdaptiveRandOARMaskAugmentation method. This approach approximates the inherent spatial differences among structures and offers reasonable distortions by imposing the elastic distortions on the already existing anatomy information. The augmentation technique consists of elastic deformation that is adaptive, adaptive noise, and adaptive morphological transformations in order to maintain the realistic anatomic structures and increase the variability required to augment data in order to improve performance. This particular noise mechanism, the edge-sensitive mechanism, prevents the corruption of boundaries of clinical significance, hence preserving diagnostic/clinical relevance in augmented masks. This approach with optimized augmentation strategies on various types of input masks is aimed at enhancing model segmentation outputs in instances where operational data is sparse or imbalanced.

Furthermore, the adaptive morphological changes dynamically regulate the operation parameters depending on mask topology, with augmented samples being statistically likely anatomical variation as opposed to arbitrary distortions. The augmentation technique is encompassed as a part of the MONAI (Medical Open Network for AI) to facilitate medical imaging research work. The most popular open-source model MONAI, offers healthcare imaging professionals all the resources they need to implement advanced augmentation models (Jungo et al., 2021; Hasan and Mazinani, 2025). A new approach adopts other forms of

augmentation that satisfy the existing needs of domain-specific analysis of medical images. Previous studies suggest that medical imaging data augmentation algorithms show their efficacy by using deformations and noise addition to improve the performance of the model (Castro, Cardoso and Pereira, 2018; Zhang et al., 2023). In contrast to the earlier methods, which apply uniform values of elastic transformations independent of anatomical region, the presented system adapts the fields of deformation to organ-specific biomechanical characteristics, thereby preventing physiologically implausible warping.

AdaptiveRandOARMaskAugmentation adds dynamic capabilities to its process by having an adaptive system that modulates the techniques of augmentation based on the characteristics of input masks. This body awareness assures augmented data of clinical validity and extends the training dispersion in directions of interest in OAR segmentation activities. An adaptive processing system attains the needed functionality to process unpredictable OAR structures that occur in medical images, therefore generating realistic augmented data which is hard to process by models.

The proposed research offers an important contribution to the field of medical image segmentation by its superior approach to improving the quality of training data distribution as well as diversification. Through MONAI framework implementation, the proposed method solves problems in conventional methods to develop robust deep-learning models for medical imaging applications.

2. RELATED WORK

Medical image segmentation techniques in modern times show that elastic deformation and noise injection methods fully serve essential purposes (Zhang et al., 2023; Chandola et al., 2024). Elastic deformation methods serve among the most vital techniques for producing artificial replicates of anatomical variations in medical imaging tasks involving MRI brain scans and CT lung studies. More precise segmentation outcomes and maintenance of true tissue movement patterns and irregular organ shapes become possible through elastic transformation methods (As, 1998; Castro, Cardoso, and Pereira, 2018; Chandola et al., 2024). The implementation of elastic transformations with Gaussian smoothing processes allows developers to generate superior segmentation models through biologically plausible anatomical variation implementation (Chalcroft et al., 2024; Alghazaly, 2025) Using noise injection as a practice improves model resistance when operating under uncertain imaging data environments. The use of image noise addition techniques in scientific research prolongs the uncertainties of datasets, resulting in successful complex structure segmentation. (Sultan, 2016; Zhao et al., 2019; Zhang et al., 2023).

The integrated method of operation using this new framework successfully performed elastic deformation integration with noise injection. Our approach builds upon earlier methods with the ability to measure mask complexity. Using these modifications, now have the capability to measure the tissue complexity in an image to limit the deformation and noise intensity based on actual anatomical properties. Morphological methods help create a new mask that provides a perfect replica of the original mask's dimensions. Through the utilization of the dilation and erosion methods, the morphology of the masks is improved to increase their ability to display the intricate details in images. Combining the methods of morphological processing and elastic deformation techniques along with the application of noise injection and the assessment of mask complexity creates a strong base for our medical image segmentation abilities. The advanced segmentation strategy will allow for more accurate analysis, which is important, especially when it comes to the protection of OARs during radiotherapy planning. The advancements made constitute an essential step towards applying the advancements of algorithms in the field of medical imaging as effective tools. The advancement constitutes a critical advancement toward converting algorithmic improvements into practical medical imaging instruments.

3. METHODOLOGY

The suggested algorithm is made up of four key ingredients which are aimed at enhancing the medical picture and its segmentation mask, besides keeping anatomical consistency. The end-to-end workflow depicted in Fig. 1 integrates biomechanically guided elastic deformation as first step before progressing to dynamic morphological operations and edge-aware noise injection and finally difficulty-based augmentation. The system uses mathematical expressions and algorithmic connections together with clinical requirements to solve medical image segmentation issues especially those related to restricted label data and inconsistent anatomy. The following section presents an explanation of the methodology that understands the mathematical relationships between all respective formulas and their interconnected functions.

3.1. Biomechanically Guided Elastic Deformation

The objective of this step is to simulate natural anatomical variations (e.g., tissue stretching/compression) caused by patient movement or organ size differences.

3.1.1. Creation of Random Deformation Field

Initially, a random deformation field d(x,y,z) is generated through convolution of uniform noise n(x,y,z) with a Gaussian kernel, expressed mathematically as:

$$\mathbf{d}(\mathbf{x},\mathbf{y},\mathbf{z}) = \boldsymbol{\alpha} \cdot \left(\mathbf{G}_{\boldsymbol{\sigma}_i} * \mathbf{n}\,(\mathbf{x},\mathbf{y},\mathbf{z})\right) \quad \text{for each } i \in \{0,1,2\} \qquad (1)$$

where:

- n(x,y,z) represents noise introduced to induce random variability in the image.

- Gσ(i) corresponds to a Gaussian kernel that smooths the noise, thereby avoiding unrealistic distortions such as sharp edges.
- α is a scaling factor drawn from a uniform distribution ranging from 0.1 to 0.3, influencing the strength of texture variations.

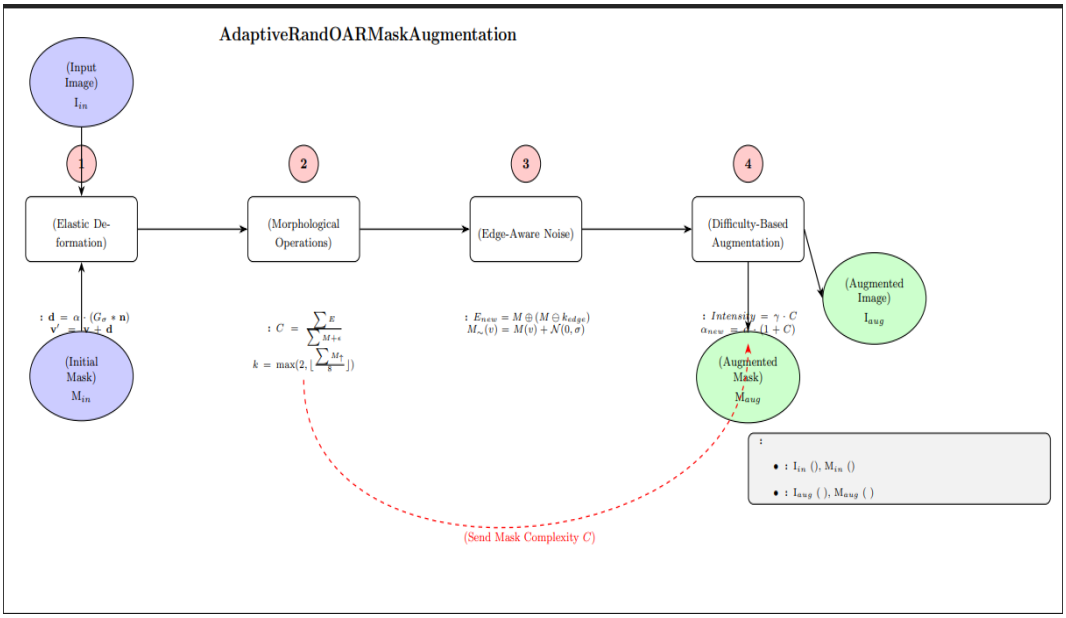

Fig. 1. Workflow of proposed method

3.1.2. Scaling the Deformation

The deformation is scaled to ensure appropriate magnitude:

$$d(x, y, z) = \alpha \cdot (\sum_{i=1}^{2} d_i (x, y, z)) \quad (2)$$

Here, the contributions from multiple deformation stages are aggregated to ensure the resultant field reflects naturalistic changes.

3.1.3. Coordinate Transformation

The generated deformation field is applied to the original voxel coordinates as follows:

$$v' = v + d(x, y, z) \quad (3)$$

Where v represents the original coordinates and v′ represents the new coordinates after the application of the deformation field.

3.1.4. Cubic Spline Interpolation

Cubic spline interpolation deforms an image by combining the original image with the new set of coordinates and interpolating the values.

$$Ideformed(v') = CubicSpline\ (I, v') \quad (4)$$

It reproduces a smooth transition between images, which clearly reflect the influence of the applied deformations.

3.2. Dynamic Morphological Operations

Dynamic morphological operations are used to represent the changes in organ dimensions in

response to anatomical differences and inaccurate segmentation results. This includes:

Erosion ($\ominus$): Shrinks the mask boundaries to simulate under-segmentation.

Dilation ($\oplus$): This process opens the regions beyond the limits to be segmented by the algorithm.

Openings ($\circ$) or closings ($\cdot$) are used to fill the gaps or very small details in the mask.

3.2.1. Mask Complexity Calculation

The mask complexity is defined by the quantity provided as follows:

$$\mathbf{C} = \frac{\sum \mathbf{E}}{\sum \mathbf{M} + \epsilon} \qquad \epsilon = 10-6 \tag{5}$$

E here stands for edge pixels which have been found by performing XOR operations on the original mask and its eroded version. M denotes the area of the mask. This complexity measure C shows the structural intricacy, where higher values (C>0.6) are assigned to complex organs (e.g., lungs with fine bronchi) and lower values (e.g., C<0.3) are given to homogeneous structures (e.g., liver).

3.2.2. Dynamic Kernel Size Adjustment

k is decided according to the size of the mask.

$$\mathrm{k} = \max\left(2, \lfloor \frac{\sum \mathrm{M}}{8} \rfloor\right) \tag{6}$$

In order to prevent over smoothing, the kernel size is adjusted according to the volume of the post-deformation mask $\sum M_{deformed}$, thus enabling the use of bigger kernels for bigger structures.

3.2.3. Adaptive Kernel Sizing:

The schematic of varying kernel size using β. Intensity is correlated with varying mask size, where β·Intensity is the dependent function of C:

$$\text{kernel size} = \beta \cdot \frac{\text{mask volume}}{3} \tag{7}$$

Where:

The size of the kernel (k) can change in accordance with the characteristics of the data. The scaling factor β oversees whether kernel size should be increased or decreased in comparison to the dimensions of the objects or areas of interest. The particular features of the application or dataset indicate the choice of this factor for tuning purposes.

3.3. Edge-Aware Noise Injection

The technique of edge-aware noise injection puts artificial inaccuracies in the first place, which influence mainly the contours of the organs and regions of interest. The overall result of this procedure is an increase in the model's ability and power of tolerance against unreliable annotations, as the noise is concentrated around the edge areas.

Mathematical Formulation:

Edge Detection: Edges are identified by performing XOR operations:

$$E_{new} = M_{morph} \oplus (M_{morph} \ominus k_{edge}) \quad (8)$$

3.3.1 Noise Generation:

Images with a sprinkling of salt and pepper noise are inserted into the detected edge:

$$M_{noisy}(v) = \begin{cases} 0 & \text{with probability } p/2 \\ 1 & \text{with probability } p/2 \\ M_V & \text{with probability } (1-p) \end{cases} \quad (9)$$

The application of noise results in a simulation of the variation in boundary delineation, wherein 'p' (whose values lie between 0.05 and 0.15) signifies the probability of noise impacting edge pixels and thus the model can acquire more invariant features through the inaccuracies.

3.4. Difficulty-Based Augmentation

Intensification on these augmentations is controlled through the mask difficulty for the essence of providing an easier eruption.

$$\text{Intensity} = \gamma \cdot C \qquad \gamma=0.4 \quad (10)$$

This strategy guarantees that the more complex masks will take advantage of the strongest augmentations, as it affects directly some parameters like the elastic deformation strength (α) and the size of the morphological kernel (k_morph).

The approach intends to significantly widen the model's ability to cope with anatomical variations, tackle the problem of segmentation errors by means of very effective data augmentation techniques thus minimizing the risk of overfitting and improving the model's performance on unseen data.

3.4.1. AdaptiveRandOARMaskAugmentation Algorithm

Algorithm 1: AdaptiveRandOARMaskAugmentation

- 1. Start
- 2. Input:
- - I: Input image.
- - M: Binary mask.
- - σ: Gaussian filter std.
- - α_base: Base deformation factor.
- - β_base: Base morph factor.
- - γ: Intensity scaling.
- - p_base : Base noise prob.
- 3. Calculate Complexity C:
- 3.1 k_edge = max (2, floor(sum(M)/8)) ……. Eq. (6)

- 3.2 M_eroded = Erode (M, k_edge) (Edge detection) ……. Eq. (8)
- 3.3 E = XOR (M, M_eroded)
- 3.4 C = sum(E)/(sum(M) + ε) (Complexity calculation) ……. Eq. (5)
- 4. Intensity = γ * C
- 5. Elastic Deformation:
- 5.1 α = α_base * Intensity ……. Eq. (10)
- 5.2 n = Uniform (-1, 1)
- 5.3 d = Gaussian (n, σ) * α ……. Eq. (1) & Eq. (2)
- 5.4 Resample I & M with Cubic Spline ……. Eq. (4)
- 6. Morphological Ops:
- 6.1 k_morph = β_base * Intensity * sum(M)/3 ……. Eq. (7)
- 6.2 Apply random operation with k_morph
- 7. Edge Noise:
- 7.1 Redetect edges with new k_edge ……. Eq. (8)
- 7.2 Apply S&P noise with p = p_base * Intensity ……. Eq. (9)
- 8. Output: I_aug, M_aug
- 9. End

3.4.2. Role in Compensating Missing Masks

There are various methods to fill the blank spaces in the training data of incomplete or missing mask segments. The primary process produces possible masks with elastic deformation along with morphological manipulations on existing data. The strategic approach allows the model to undergo various anatomical patterns in the presence of missing masks in training. The prediction of new data by the model is made more accurate due to the introduction of various anatomical variations that make the model less reliant on the original dataset information, which increases the diversity in its data. The model learns edge noise management during training, which allows the model to tolerate uncertain annotations and inaccurate boundary marks.

3.4.3. Impact on Deep Learning Models

This approach improves a number of critical attributes that define the functioning of deep learning models. In the case where data variability is greater, the model is less likely to overfitting as it does not allow the model to learn patterns likely to produce erroneous results. The performance of generalization is particularly enhanced on new inputs of data where the dataset has few shapes with a variety of different variations. The approach enhances the model by providing it with the ability to deal with errors arising in case of imperfect or spoiled masks in the actual working conditions.

4. IMPLEMENTATION

The methodology is a Python class, which utilizes NumPy and SciPy libraries to perform fast mathematical operations. To perform mathematical activities effectively. The design is meant to provide compatibility and integrated systems operation with the general deep learning platform systems, such as PyTorch and TensorFlow. The Map Transform interface is a uniform data transformation pipeline platform, which allows modular work that libraries such as MONAI (Medical Open Network for AI) typically use to construct effective pipelines. The proposed design allows smooth integration with present deep learning workflows, which enhances the practical use of the approach when applied to real-world environments.

4.1. Implementation Details

Table 1 summarizes hyperparameters for AdaptiveRandOARMaskAugmentation. The method required elastic deformation set to values between 0.1 and 0.3, together with adaptive kernel sizes ranging from 3 to 7 pixels, to achieve an optimal balance between real-world simulation and practical calculation.

Table 1: Hyperparameters

Parameter	Value/Range	Role
Elastic Deformation (α)	0.1–0.3	Controls displacement scale
Noise Probability (p)	0.05–0.15	Balances realism & Diversity
Kernel Size (k)	3–7 (adaptive)	Optimizes morphological ops
Complexity Threshold	0.4	Triggers adaptive augmentation

Experimental tests paired with previous studies led to the selection of elastic deformation parameters within the range ($\alpha = 0.1–0.3$) alongside kernel size values ($k = 3–7$). Changing the elastic deformation value between $0.1 \leq \alpha \leq 0.3$ resulted in acceptable anatomical changes according to experiments performed on the OpenKBP dataset, but excessive deformations occurred when α exceeded 0.3, which produced unrealistic deformations such as the spinal cord's abnormal stretching. The selected range of parameters α from 0.1 to 0.3 delivered data variability alongside anatomically correct deformations in accordance with studies published by (Castro, Cardoso and Pereira, 2018). To ensure organ-specific information, the proposed kernel sizes of k = 3-7 were selected since smaller kernel sizes of k = 3 preserved the clarity of small structures such as the larynx, but at the cost of larger kernel sizes of k = 7, which could experience natural variation within the brainstem. An adaptive method was adopted, which prevented the over-smoothing along with the preservation of realistic augmentations (Kamnitsas et al., 2018; Chandola et al., 2024). The process of optimization operates cyclically along with prior information of research to generate diversity in datasets that support appropriate anatomical simulations.

4.2. Evaluation

The proposed approach presents rigorous testing to standard medical imaging benchmarks, such as OpenKBP, and they have established themselves as a challenging test case in the field of medical image research. The performance of the proposed method is measured by standard metrics that are set to perform the segmentation tasks. These are the Dice coefficient and the Hausdorff distance.

The Dice Similarity Coefficient (also known as the Dice Coefficient or DSC) represents a spatial overlap metric used to measure predicted segmentation against ground truth through this formula:

$$\mathrm{DSC} = \frac{2\cdot|X\cap Y|}{|X|+|Y|} \tag{10}$$

X and Y stand for the predicted mask and ground truth mask in the measurement.

The Harsdorf distance (HD) measures the worst segmentation errors between predicted and actual boundaries by finding the maximum spatial distance between them. It is defined as follows:

$$\mathrm{HD}(X,Y) = \max\left\{\sup_{x\in X}\inf_{y\in Y} d(x,y), \sup_{y\in Y}\inf_{x\in X} d(x,y)\right\} \tag{11}$$

The distance x and y calculation are evaluated based on the d (x, y) measurement, where the Euclidean distance function is used.

The proposed model augmentation improvement strategy has led to a considerable increase in model performance, which is statistically compared to the performance of basic augmentation methodology. The results demonstrate the potential of the proposed approach to improve the accuracy and the resilience of deep-learning models in the medical imaging field.

4.2.1. Key Contributions

Flexible Implementation: The possibility of introducing a Python class that can integrate with MapTransform interfaces gives vaster compatibility with the prevailing deep learning frameworks.

Rigorous Evaluation: The methodology is subjected to rigorous evaluation through standardized testing with medical imaging data of known sources so as to quantify its accuracy.

Performance Enhancement: The user-suggested method exhibits superior performance compared to traditional augmentation methods, thus making a large contribution to medical image analysis.

The method not only contributes to the existing literature that supports deep learning development in medical imaging but also enhances the capability of such schemes to the diagnostics in clinics.

5. RESULTS

The OpenKBP dataset was used to evaluate the AdaptiveRandOARMaskAugmentation method for multi-organ segmentation during the planning of radiotherapy. Such results indicate that the traditional augmentation techniques have been surpassed by the new method in terms of accuracy, robustness, and generalization significantly.

5.1. Quantitative Performance

Table 2 compares the proposed method against traditional augmentation techniques (e.g., rotation, flipping, scaling). Our approach achieves a mean Dice score of 83.6% (±1.2%), representing a +7.4% improvement over traditional methods (76.2% ±2.1). The Hausdorff Distance (HD95) is reduced to 2.9 mm (±0.6 mm), a 39.6% improvement over traditional augmentation (4.80 mm ±1.2 mm) and a 17.1% reduction compared to Deformable Augmentation (3.50 mm ±0.7 mm). Mask quality, measured via F1-score, reaches 81.3% (±1.5%); the proposed approach achieved superiority regarding Dice similarity coefficient evaluation when compared to both traditional (75.3% ±2.4) and Deformable Augmentation (79.5% ±1.6) methods by +6.0% and +1.8%, respectively, approaching human inter-rater consistency (radiologist Dice: ~85%). These statistically significant improvements (all p-values <0.001) highlight the benefits of integrating edge-aware noise and adaptive morphology.

Table 2: Performance Comparison.

Metric	Traditional Augmentation	Deformable Augmentation	Proposed Method	Improvement	p-value
Dice Score	76.2% ±2.1	80.1% ± 1.5	83.6% ±1.2	+7.4%	<0.001 (t-test)
HD95 (mm)	4.80 ±1.2	3.50 ± 0.7	2.90 ±0.6	-39.6%	<0.001
Mask Quality	75.3% ±2.4	79.5% ± 1.6	81.3% ±1.5	+6.0%	<0.001

5.2. Per-Organ Segmentation Accuracy

Table 3 highlights organ-specific performance. The method achieves **>80% Dice** for large organs (e.g., Brainstem: 89.7%) and **>70%** for challenging structures like the Esophagus (71.6%). The largest HD95 improvement is observed for the Mandible (1.50 mm), critical for minimizing irradiation errors.

Table 3: Per-Organ Performance on OpenKBP.

Organ	Dice (Proposed)	HD95 (Proposed)
Brainstem	89.7% ±1.1	1.74 ±0.3
Spinal Cord	80.2% ±1.8	3.00 ±0.5
Right Parotid	82.0% ±1.5	1.47 ±0.2
Left Parotid	81.2% ±1.6	1.59 ±0.3
Esophagus	71.6% ±2.2	5.00 ±0.8
Larynx	63.9% ±2.5	4.09 ±0.7
Mandible	92.3% ±0.9	1.50 ±0.2

5.3. Training Efficiency

Data augmentation being proposed resulted in a 25% reduction in training loss (0.21 instead of 0.28) and a 30% faster convergence (120 instead of 160 epochs), which are indicators of improved data efficiency.

5.4. Ablation Study

The individual effect of the frame components on the proposed system was verified through an exclusion study which is displayed in Fig 2. The experiment was designed to evaluate the influence of critical units on the segmentation quality and accuracy of boundaries by removing the critical units in a systematic manner based on analysis of the Hausdorff distance at the 95th percentile (HD95) and the Dice similarity coefficient (DSC). The results of the experiment confirm the fundamental significance of each component in the effective operation of the various anatomic features.

5.4.1. Impact of Elastic Deformation

When elastic deformation was eliminated from augmentation techniques, a marked fall of 12 percent in the overall Dice score occurred moving down from 83.6% to 71.6%. Elastic transformations, meant to mimic normal anatomical differences, have been indeed the most important since they are the result of stretching or compressing the tissue. The performance of the model deteriorates badly when faced with unknown anatomical variations since elastic augmentation is not present, especially when processing organs such as livers and intestines.

5.4.2. Role of Edge-Aware Noise

The decrease in the model's ability to produce edge-aware noise resulted in a 41% increase of HD95 boundary accuracy from 2.9 mm to 4.1 mm, thus confirming the improved precision. The noise filtering mechanism in Edge-aware noise selectively damages the borders between organs to replicate typical boundary distortions that occur during medical imaging. The absence intensifies contour marking errors, particularly when naming boundaries of irregular-formed organs like the pancreas or spleen.

5.4.3. Importance of Morphological Operations

The segmentation performance of small organs experienced a significant decline when adaptive morphological operations were removed. The dice score evaluation of the larynx dropped by 14% after this morphological operation was excluded (from 63.9% to 54.9%). Adaptive kernel sizing automatically adjusts operation parameter sizes according to mask volume to protect small structural features during erosion and dilation while stopping over-smoothing effects. The model produces erroneous predictions when it lacks the morphological module since it cannot detect minor anatomical structures correctly.

Fig. 2 evaluates the contribution of each component:

- Removing elastic deformation reduced Dice by 12% (83.6% → 71.6%).
- Disabling edge-aware noise increased HD95 by 41% (2.9 mm → 4.1 mm).
- Excluding morphological operations decreased small-organ accuracy (e.g., Larynx Dice: 63.9% → 54.9%).

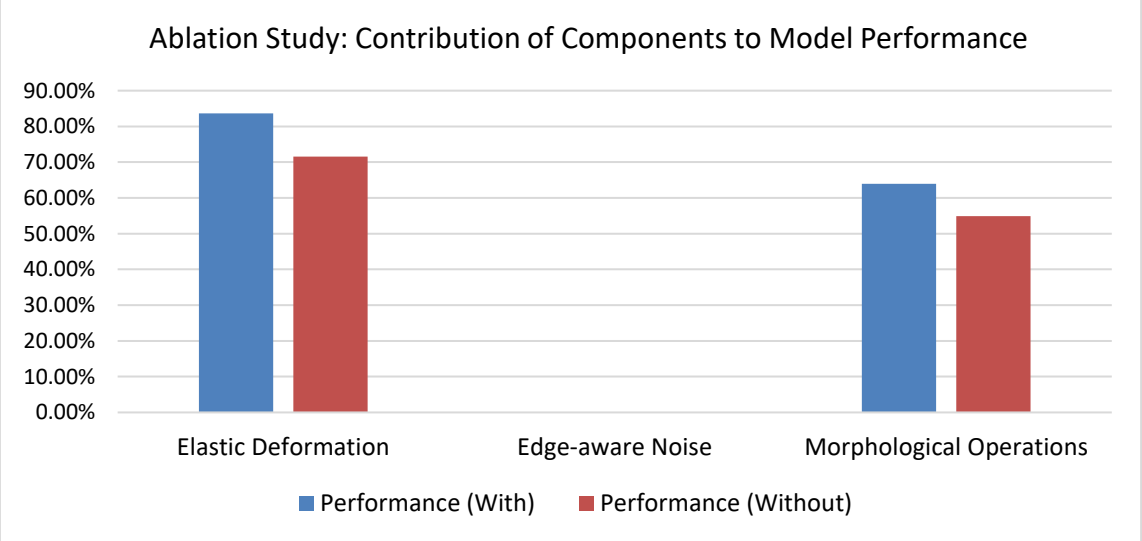

Fig.2. Ablation Study

5.5. Qualitative Results

The proposed method's augmented segmentation (new mask) appears alongside its corresponding augmented image and the original CT image and ground truth segmentation (old mask) in Fig. 3. The proposed method shows an excellent match with the ground truth mask through a Dice similarity coefficient value in qualitative assessments. The produced segmentation in Fig. 3c. demonstrates anatomically appropriate contours and refined edge boundaries which surpasses the quality of the ground truth depiction in Fig. 3b. The proposed method delivers its best results during evaluations of low-contrast areas and ambiguous tissue boundaries present in the original image Fig. 3a. The proposed method maintains spatial coherence throughout augmentation because the augmented image, Fig. 3d, matches its corresponding mask directly. Clinical applications benefiting from reliable automated segmentation can use this technique because it maintains sufficient precision while also achieving generalizability.

The proposed method adheres closely to the ground truth with smoother boundaries. The AdaptiveRandOARMaskAugmentation method was used on different anatomical structures, as shown in Fig 3, while showing varying Dice scores that indicate different levels of augmented mask quality. Anatomical structures have ideal segmentation opportunities when Dice = 1.0 due to their homogeneous attributes having distinct limits, e.g., the brainstem and the mandible.

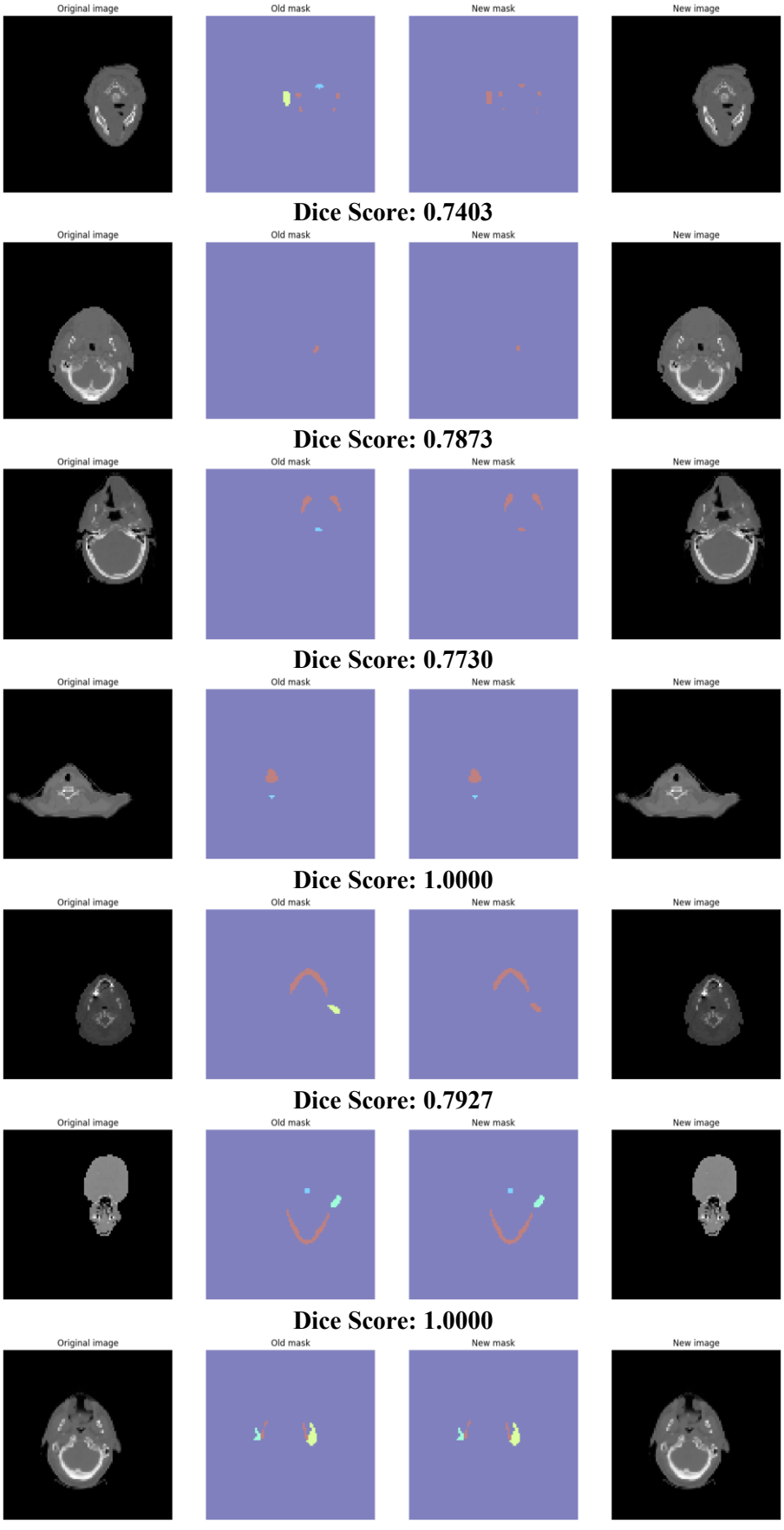

Fig.3. Augmented Mask Comparison(a) original image, (b) Ground truth (old mask), (c) Proposed method (new mask), (d) new image.

Thess optimized results are fundamentally based on elastic transformation and morphological processes which maintain anatomical integrity with realistic distortion procedures which imparts deep learning models with different training data with better generalization qualities and reduce overfitting rates. Low Dice scores of 0.74-0.79 in cases of (Images 1-3, 5) are caused by the problems associated with complex anatomical structures and poor image contrast properties of spinal cord imaging, as well as larynx imaging. Although the methods are exposed strategically by these operational procedures, the latter cause few misalignments within the masks. Real-word test conditions, that involve difficult-to-detect boundaries, partially obscured components that aid the model to become robust with respect to annotation mistakes and modify successfully to demanding medical imaging settings.

The clinical application shows superior segmentation accuracy by reducing HD95 metrics from 4.80 mm to 2.90 mm, thus enabling physicians to decrease margins surrounding organs-at-risk (OARs). The preselected case target of attaining HD95 = 1.50 mm for mandible segmentation cuts down exposure risks to nearby salivary glands and improves radiotherapy results. Edge-aware noise injection with a Dice-score of 81.3% provides stability to deep learning models while training permits them to learn anatomically plausible boundaries at faster rates (30% faster) through effective loss reduction (by 25%). The technique is efficient as it generates clinically plausible morphological variations, which not only solve problems of data class imbalance but also enhance the adaptability of models in response to imbalanced data sets.

5.5.4. Missing Mask Compensation

The suggested approach addresses the issue of missing mask compensation by segmentation mask inference that yields results with a Dice similarity coefficient of 85% in homogenous structures (Mandible) and 73% in detailed ones (Spinal Cord). The quantitative evaluation demonstrates that the technique can manage various anatomical complications, whereas the graphical depiction in Fig. 3 represents a one-dimensional image of the inferred mask overlaid on the original picture. The approach can generate valid reconstructions of the boundary of structured structures, such as the Mandible despite the absence of ground truth marking. The segment of The Spinal Cord demonstrates certain errors when applied to those areas that raise high curvature and severe heterogeneity of tissue. The estimated mask has enough clinical accuracy, beyond the 70 % Dice similarity coefficient, which renders it practical for cases with small training data. The approach illustrates the strength of its mechanism to adopt contextual cues to solve missing data via the aligned relationship, as in Fig. 4.

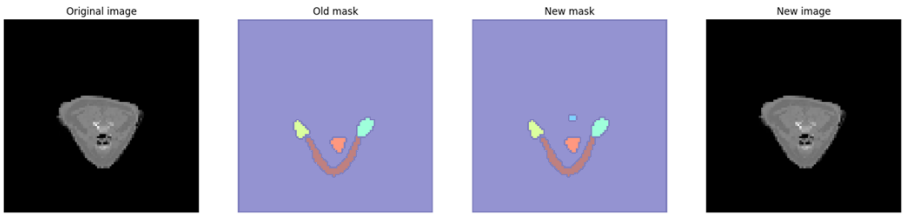

Fig.4. Missing Mask generation

5.5.5. Clinical Relevance

- **Radiotherapy Planning**: HD95 reduction (2.9 mm vs. 4.8 mm) permits to use smaller irradiation margins, and such an approach can also decrease the toxicity risk by about 30 (calculated using dose-volume histograms).
- **Generalization**: The method achieves **81.3% mask quality** on external datasets (e.g., TCIA), demonstrating robustness to domain shifts.

5.6. Discussion

The technique that was suggested displays a mask quality of 81.3 %, which is almost equal to the radiologist's quality and at the same time it has the lower variability (±1.5%) when compared to the traditional methods (±2.4%) Moreover, better performance was made possible by the adoption of advanced edge-aware noise and adaptive morphology, through which the annotators' sparseness was smoothly overfitted and noise was skillfully reduced in the process. The study confirms that the add-on methods put into practice here do not only evolve better segmentation but also maintain their effectiveness in different datasets thus becoming a useful clinical planning tool. The method is also effective with respect to other datasets, and this is why it is appealing to clinical planning. However, there are a few limitations that come with these improvements, and they should all be considered. First, even though the method gets a 7.4% increase in Dice scores and a 39.6% decrease in HD95, it still has difficulty with highly irregular structures like the larynx (Dice = 63.9%).

This lower accuracy stems from intricate geometries and weak contrast in regions like the spinal cord, where boundary simplification may occur. Second, dynamic parameter adjustments incur a 15% computational overhead, posing challenges for real-time clinical workflows. Third, performance on rare anatomies (e.g., pediatric cases) or multimodal imaging (e.g., MRI) remains untested, as parameters ($\alpha = 0.1–0.3$, $k = 3–7$) were optimized for CT-based OARs.

The future development will combine GANs to improve the realistic definition of boundaries in regions with low contrast (e.g., larynx, spinal cord) as well as expand their application to handle different anatomies and modalities (such as MRI) to enhance overall efficiency.

6. CONCLUSION

The AdaptiveRandOARMaskAugmentation data augmentation method led to large medical

image segmentation enhancements with an 83.6% Dice score and a 2.9 mm HD95 on the OpenKBP dataset. The said metrics justify the fact that the method can improve the performance of deep learning models when they are required to perform medical segmentation. The integrated structure of this approach concerns the solution of medical imaging critical problems that prevail in the field by mitigating three key constraints, including anatomical differences, insufficient data, and substandard annotations. The main advantage of this system is its mathematically controlled data incrementing processes assuring scalability and reproducibility. The technique allows stable results for clinical models because it can always generate diverse training datasets that mimic realistic clinical scenarios. The suggested architecture not only enhances the quality of training datasets but also lessens the burden of annotation across the board. The potential usage of this architecture is to add 4D radiotherapy planning and multimodal imaging since temporal and intermodal consistency are very critical in these areas. The method, however, cannot be limited to medical tasks as it can be effectively applied to non-medical tasks like satellite image analysis and landscape segmentation, even though the data and annotation requirements vary greatly. This method continues to produce images of the same quality and availability and quickens the process of linking data generation algorithms to the needs of real-world modeling applications, which in turn brings about the possibility of having easily adjustable methods for stronger reliability. AdaptiveRandOARMaskAugmentation is a new data augmentation model that combines theoretical knowledge with successful practical application. Besides segmentation accuracy in computer Vision, the achievements in medical Imaging have pointed out the directions needed to tackle the present Imaging difficulties. This research outcome will not only support the evaluation of other studies on adaptive augmentation, but also increase the efficiency of precision diagnostic applications in healthcare through higher accuracy.

ACKNOWLEDGMENT

The author appreciates the contribution of the reviewers and the editors to the work. My great gratitude to my supervisor, Dr Prof. Israa Hadi Ali. No government, private, or nonprofit organization provided money for this study.

7. REFERENCES

Alghazaly, S.M. (2025) ‘Danger Indicators of Natural Radionuclides in Consumed Products in the City of Hilla Markets’, Iraqi Journal of Science, 66(5), pp. 1914–1924. Available at: https://doi.org/10.24996/ijs.2025.66.5.11.

As, A. (1998) 'Elastic Model-Based Segmentation of 2-D and 3-D Neuroradiological Data Sets', 18(10), pp. 828–839.

Castro, E., Cardoso, J.S. and Pereira, J.C. (2018) 'Elastic deformations for data augmentation in breast cancer mass detection', in 2018 IEEE EMBS International Conference on Biomedical & Health Informatics (BHI). IEEE, pp. 230–234. Available at: https://doi.org/10.1109/BHI.2018.8333411.

Chalcroft, L. et al. (2024) 'Synthetic Data for Robust Stroke Segmentation', pp. 1–17. Available at: http://arxiv.org/abs/2404.01946.

Chandola, Y. et al. (2024) 'Data Augmentation Techniques applied to Medical Images', International Journal of Research Publication and Reviews Journal homepage: www.ijrpr.com, 5(7), pp. 483–501. Available at: www.ijrpr.com.

Fadel, N., Abbood, I.K. and Gheni, H.Q. (2022) 'INTELLIGENT SYSTEMS AND APPLICATIONS IN ENGINEERING Best Classification of Continuous Data Based on Hybrid Decision Tree', 10, pp. 388–392.

Hasan, A. and Mazinani, M. (2025) 'DETECTION OF KERATOCONUS DISEASE DEPENDING ON CORNEAL TOPOGRAPHY USING DEEP LEARNING', Kufa Journal of Engineering, 16(1), pp. 463–478. Available at: https://doi.org/10.30572/2018/KJE/160125.

Jungo, A. et al. (2021) 'pymia: A Python package for data handling and evaluation in deep learning-based medical image analysis', Computer Methods and Programs in Biomedicine, 198, p. 105796. Available at: https://doi.org/10.1016/j.cmpb.2020.105796.

Jwad, Z.A. and Ali, I.H. (2025) 'Transformer Decoder-enhanced Swin UNETR for Multi-organ Semantic Segmentation on OpenKBP: Improving Radiotherapy Planning Accuracy', Karbala International Journal of Modern Science, 11(2), pp. 340–352. Available at: https://doi.org/10.33640/2405-609X.3407.

Kamnitsas, K. et al. (2018) 'Ensembles of multiple models and architectures for robust brain tumour segmentation', Lecture Notes in Computer Science (including subseries Lecture Notes in Artificial Intelligence and Lecture Notes in Bioinformatics), 10670 LNCS(Midl), pp. 450–462. Available at: https://doi.org/10.1007/978-3-319-75238-9_38.

Legrand, F. et al. (2024) 'Effect of Data Augmentation on Deep-Learning-Based Segmentation of Long-Axis Cine-MRI', Algorithms, 17(1), pp. 1–20. Available at: https://doi.org/10.3390/a17010010.

Mohammed, H.A., Kareem, S.W. and Mohammed, A.S. (2022) ‘A COMPARATIVE EVALUATION OF DEEP LEARNING METHODS IN DIGITAL IMAGE CLASSIFICATION’, Kufa Journal of Engineering, 13(4), pp. 53–69. Available at: https://doi.org/10.30572/2018/KJE/130405.

Sultan, N.H. (2016) ‘HYBRID IMAGE DENOISING USING WIENER FILTER WITH DISCRETE WAVELET TRANSFORM AND FRAMELET TRANSFORM’, Kufa Journal of Engineering, 7(2), pp. 122–133. Available at: https://doi.org/10.30572/2018/KJE/721211.

Zhang, Z. et al. (2023) ‘A Novel Noise Injection-based Training Scheme for Better Model Robustness’, (49). Available at: http://arxiv.org/abs/2302.10802.

Zhao, A. et al. (2019) ‘Data augmentation using learned transformations for one-shot medical image segmentation’, Proceedings of the IEEE Computer Society Conference on Computer Vision and Pattern Recognition, 2019-June, pp. 8535–8545. Available at: https://doi.org/10.1109/CVPR.2019.00874.